7

Programmable Microscopy

Tobias Haist[1], Malte Hasler[1], Wolfang Osten[1] and Michal Baranek[2]
[1]*Institute für Technische Optik, Universität Stuttgart, Germany*
[2]*Department of Optics, Palacky University Olomouc, Czech Republic*

7.1 Introduction

Today, a huge number of imaging methods for the investigation of microscopic specimens are available and most of these methods have some parameters that will strongly affect imaging. For microscope users, it is–at least most of the time–impossible to chose the perfect combination for the imaging task at hand.

Programmable microscopy is a technique that allows one to easily switch at high speed between these different imaging methods. If we denote the imaging method by p_0 and its parameters by p_1, p_2, ... "optimized imaging" means that the overall set of parameters $p(p_0, p_1, p_2, ...)$ leads to the "best" suited image to a given task.

In a multi-image context we can use multiple images obtained with different parameters p in order to find a good, or even perfect, imaging result. Moreover, we might use the images obtained with different parameters in order to generate one optimized image by digital post-processing.

Up until now, only a few very rudimentary examples of such approaches have been realized but we think that this methodology might lead to the next generation of powerful microscopes. In order to realize such methods, fortunately, not much hardware is necessary. It is enough to incorporate programmable elements into the optical train of the microscope.

The preferred approach is to use spatial light modulators (SLMs) in the illumination and/or imaging path of the microscope. This has been proposed in the past for a lot of different, interesting applications. Particularly within the last 10 years a lot of methods have been investigated, mainly due to the availability of high quality spatial light modulators. Important methods are optical micromanipulation (Eriksen *et al*. 2002; Grier 2003; Hayasaki *et al*. 1999; Reicherter *et al*. 1999), multi-photon microscopy (Nikolenko *et al*. 2008; Peterka *et al*. 2010; Qin *et al*. 2012), structured-light illumination (Chang *et al*. 2009; Choi and Kim 2012; Hussain and Campos 2013; Wang *et al*. 2009), Raman and coherent anti-Stokes

Multi-dimensional Imaging, First Edition. Edited by Bahram Javidi, Enrique Tajahuerce and Pedro Andrés.

Raman imaging (Jesacher *et al*. 2011), point-spread function engineering (Kenny *et al*. 2012), interference microscopy (Schausberger *et al*. 2010), microscopic spectroscopy (Pham *et al*. 2012), stereo microscopy (Hasler *et al*. 2012; Lee *et al*. 2013), holographic microscopy (Mico *et al*. 2010; Valencia and Moliner 2010), phase contrast imaging (Bernet *et al*. 2006; Glückstad and Mogensen 2001; Khan *et al*. 2011; Kim and Popescu 2011; Maurer *et al*. 2011; McIntyre *et al*. 2009a), confocal imaging (Heintzmann *et al*. 2001), lithography (Gittard *et al*. 2011; Haist *et al*. 1999; Jesacher and Booth 2010; Zhou *et al*. 2013), multispot-imaging and spectroscopy (Nikolenko *et al*. 2010; Pham *et al*. 2012; Shao *et al*. 2012), and aberration correction (Débarre *et al*. 2009; Haist *et al*. 2008; Reicherter *et al*. 2004; Scrimgeour and Curtis 2012).

The main advantage of this sort of programmable microscopy is that we can change from one imaging method to the next very fast, always using the same image sensor. Therefore, different information about a specimen can be obtained and the multiple images can be fruitfully combined into one final image.

In this contribution we concentrate on approaches that use a spatial light modulator in the imaging path. We explain the optical design considerations that have to be taken into account when implementing programmable microscopy and we describe the current most important applications, aberration correction, and phase contrast imaging.

7.2 Optical Design Considerations and Some Typical Setups

A sketch of a typical setup used to manipulate the imaging path of a microscope is shown in Fig. 7.1. The spatial light modulator is ideally located in a plane conjugate to the exit pupil of the microscope objective lens (MO). For a conventional MO the exit pupil is inside the MO, therefore, some sort of imaging is necessary. Most often a telescopic imaging system is employed because it preserves the wavefront curvature (a plane wave on the SLM leads to a plane wave in the pupil of the MO). Also, it can easily be integrated into the collimated path of most modern research microscopes. With such an approach the SLM is located in a Fourier plane of the object, therefore, a filter written into the SLM can be regarded as a Fourier hologram.

For this case of telescopic imaging one chooses the magnification of the telescope $|\beta'| = f_2/f_1 = D_{SLM}/D_{MO}$ based on the effective aperture of the SLM D_{SLM} and the diameter of the pupil of the MO D_{MO}. If the system is used with different objective lenses, a zoom system can be employed or one has to find a compromise concerning the usable number of pixels and the usable numerical aperture of the microscope. This necessary number of pixels depends on the details of the application, especially on the carrier frequency that is used.

In practice, light modulators are never perfect. Deviations in modulation characteristics lead to unwanted diffraction orders and, therefore, to a loss of contrast in the image plane due to the overlay of multiple, modified, and shifted copies of the object. Therefore, it is advantageous to superimpose a carrier frequency to the filter. This separates the filtered image (positive first diffraction order) from other components (e.g., zeroth diffraction order). This means that the Fourier holograms written into the SLM are off-axis holograms. The basic idea is shown in Fig. 7.2.

On the other hand, a high carrier frequency leads to a reduced diffraction efficiency and increased fringing field effects (see Section 7.3). Additionally, as the response curve of the SLM depends strongly on the wavelength, the display has to be characterized carefully to

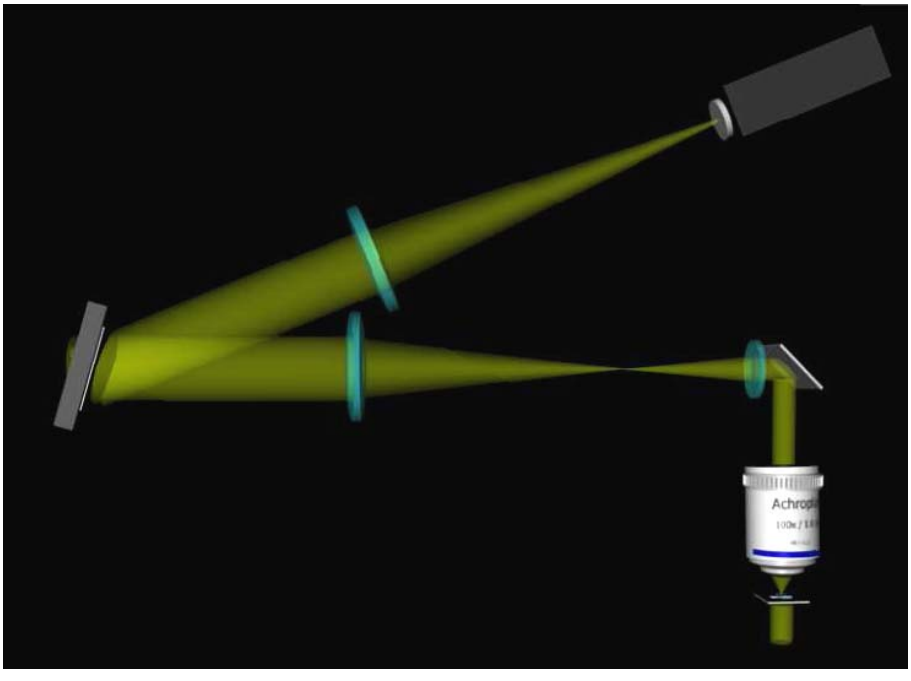

Figure 7.1 Basic setup for using a spatial light modulator (SLM) in the imaging path of a programmable microscope. The pupil of the microscope objective lens is imaged onto the SLM using a Kepler telescope

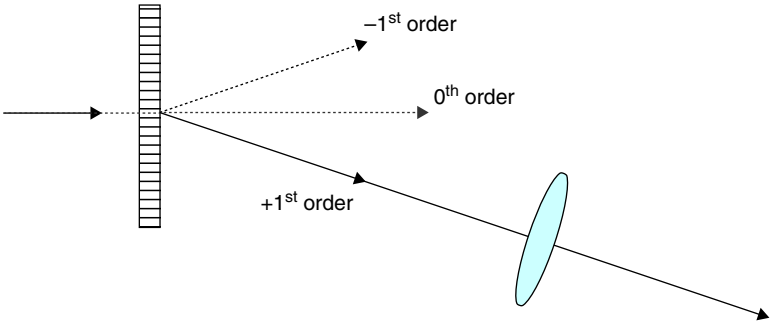

Figure 7.2 A carrier frequency approach that can be employed in order to seperate unwanted diffraction orders of the modulator from the desired order (here: positive first order)

minimize the loss of light. In practice, a carrier frequency of four gray levels is a good compromise but the usable object field is reduced when SLMs with a limited space bandwidth are used because the angular separation of the different orders due to the carrier frequency effectively limits the field of view.

One should keep in mind that such an approach is only necessary due to the non-ideal modulation behavior of the SLM (compare Section 7.3).

It is also possible to try to eliminate the images due to unwanted diffraction orders by post-processing of multiple images. We explain this idea based on the unwanted zeroth order of the hologram. Without special optimization precautions (Liang *et al*. 2012) this order will be present when using commercial SLMs. Two images are recorded with different filters displayed on the SLM. One image with the SLM set to a constant phase and the other incorporating a filter, for example, one with a small carrier frequency. If one subtracts the (correctly normalized) images it is possible to eliminate the disturbing order (see Fig. 7.3).

For this sort of imaging without strong carrier frequency, incoherent light has to be used because otherwise, of course, the behavior is nonlinear in intensity and, therefore, the subtraction would not eliminate the unwanted images.

Typically, most applications that have been published up until now use coherent light for imaging. However, it is well known that in microscopy, coherence leads to problems most of the time, namely speckles, other interference-related disturbances and artifacts (e.g., problems due to dust on an optical surface). It is possible to use averaging approaches, for example, rotating diffusers or vibrating modulators, or even multiple recordings using different SLM addressings, in order to avoid these problems.

Of course, the more straightforward approach is to reduce the coherence of the illumination. To this end, in most of our current programmable imaging setups we use LEDs in combination with bandpass filters. The bandpass is necessary because the dispersion at the carrier frequency of the gratings written into the SLM leads to chromatic aberrations in the image plane. The tolerable spectral width (and therefore the coherence length) has to be computed based on the geometry of the imaging system (magnification, pixel size of the sensor, SLM position) and the filters or gratings that will be written into the SLM. An interesting alternative is to use an additional grating in order to cancel the dispersion as described by Steiger *et al*. (2012).

It is also possible to vary the position of the SLM so that it is not located conjugate to the pupil of the MO. Depending on the diameters in the system and the location of the MO pupil this might make it possible to strongly reduce the overall size of the system. In this case, however, one has to carefully analyze the system with respect to vignetting (vignetting starts if

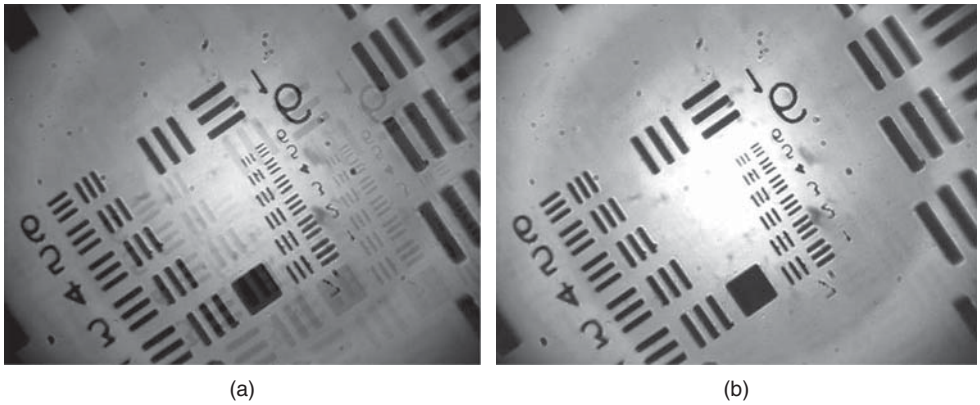

(a) (b)

Figure 7.3 Subtraction of three images which have been obtained with and without filters written into the SLM leads to elimination of the unwanted diffraction order. (a) single image, (b) image obtained by subtracting a zeroth-order image and a minus first order image

the marginal rays of an on-axis object point fall onto the edge of the SLM) and the illumination might be modified.

For most phase-contrast methods (e.g., Zernike-based methods or dark field, see Section 7.5) it is necessary that the light source is conjugate to the SLM. For a typical Köhler-type illumination and having the SLM located in the Fourier plane of the specimen this is automatically the case. But shorter designs are possible if one does not use a perfect Köhler geometry. Of course, the illumination should be more or less homogeneous in the object plane and the illumination source should be imaged onto the SLM. The numerical aperture of the illumination is limited but this is only a restriction if extremely good resolutions are to be achieved.

Figure 7.4 shows one such design. Like all of our current setups, it employs a HDTV LCOS SLM (Holoeye Pluto, 1920×1080 pixels, 8 µm pixel pitch, compare Section 7.3) and a 1/3'' CCD camera (SVS-Vistek eco204, 1024×768 pixels). For the SLM to work optimally it is necessary to ensure polarization of the incoming beam.

The 16:9 format of the SLM is only used within a circular pupil for this setup. For applications that are very demanding concerning field of view (typically proportional to the space-bandwidth product of the modulator) an anamorphotic imaging system can be used.

In Fig. 7.5 a more complex setup is shown that is not optimized concerning size. Compared to the basic setup this system allows us to chose three different types of illumination (transmission homogeneous, transmission structured, reflection homogeneous (EPI)). The homogeneous transmission illumination employs a classical Köhler illumination based on a high power LED (OSRAM Diamond Dragon, $\lambda = 632$ nm with a 1 nm bandwidth filter and a Zeiss $10 \times \mathrm{NA} = 0.22$ lens). The Köhler illumination in reflection is basically the same, except for the different wavelength of $\lambda = 532$ nm. The wavelength filter is of course necessary in this case as well. Additionally a beamsplitter will have to divide illumination and imaging pathways.

The third option employs a slightly more complicated illumination using a laser. Since the wavefronts on the SLM generally are circular, and the SLM has a format of 16:9, a large portion will, in single use, remain unoccupied. This part is used for controlling the laser illumination.

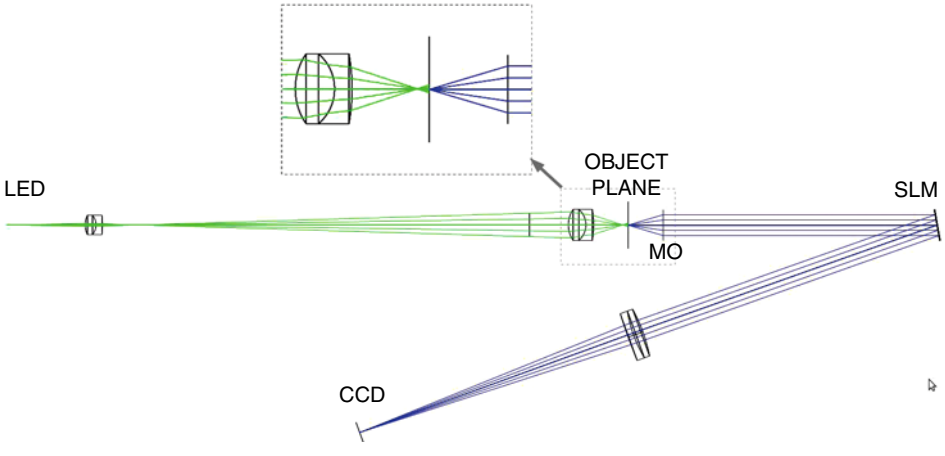

Figure 7.4 Principle of compact setup with a non-Köehler illumination. The illumination source is imaged onto the SLM. The pupil of the MO is not imaged onto the SLM

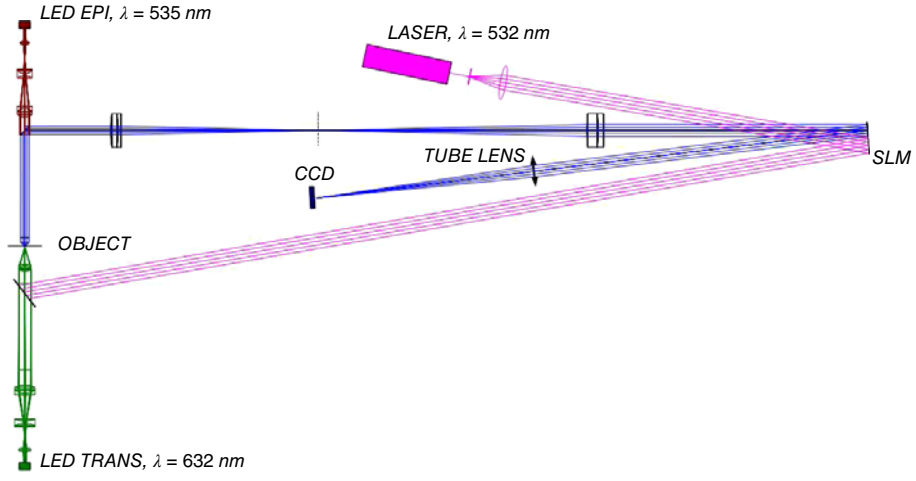

Figure 7.5 Extended setup with programmable imaging and illumination. Three different illuminations are present. The center path shows the imaging

The laser is expanded and propagates via the SLM and by means of a Kepler telescope to the illumination optics.

7.3 Liquid Crystal Spatial Light Modulator

Of course, the core element of a programmable microscope is the spatial light modulator. For the most common applications (the ones that we show in this chapter), it is beneficial to locate this modulator in a plane conjugate to the pupil or in a plane that is at least separated from planes conjugate to the object. And in this case it is then an advantage to be able to modulate the phase.

For applications where only the correction of aberrations is required, non-pixelated elements (most often: membrane mirrors: Paterson *et al*. 2000; Sherman *et al*. 2002) are the elements of choice. In this case a relatively broad spectral range can be used, no unwanted diffraction orders will occur and the light efficiency is close to 100%. Unfortunately, such elements are still quite sensitive to damage and external disturbances, can only be used for correcting low order aberrations with small amplitudes, need high voltages, and the overall system (addressing and modulation) is expensive. A large variety of other specialized AO-modulators like membrane, bimorph, piezoelectric, or electrostatic mirrors, and low-resolution liquid crystal modulators have been and still are being developed: see Tyson (1998) and Olivier (2007) for an overview. But the cost of these modulators is considerably above what can be employed in a commercial research microscope.

For applications where more complicated modulation patterns are necessary, pixelated elements are used. Amplitude-modulation certainly is possible but leads to symmetric diffraction orders and a strong loss of light. Therefore, the element of choice for most applications is a liquid crystal phase modulator with a high fill factor. Most often reflective parallel aligned liquid-crystal on silicon (LCoS) modulators are used because they offer large space-bandwidth-products in combination with high efficiency at a reasonable price.

When using such an element one should be aware of their behavior when modulating light. We do not want to go into detail here (see Lazarev *et al*. 2012; Zwick *et al*. 2010) but want to point out the most important things that might have to be considered:

- Modulation properties (variation of amplitude, phase, and polarization depending on gray level),
- number and geometry of the pixels (e.g., fill factor, space-bandwidth product, transfer function of the pixels),
- additional factors that lead to a loss of contrast (scattering, absorption, coatings),
- discritization and quantization,
- fringing field effects (electrical and optical crosstalk),
- variation with time (e.g., due to pixel refresh and PWM-addressing),
- temperature dependence (e.g., temperature increase due to the energy of the incident light),
- dependence on polarization,
- reconstruction geometry, including incidence angle.

To make things even more complicated, many of these factors depend-, in a non-trivial way-, on secondary factors (e.g., characteristic of the graphics board used for addressing the SLM). Figure 7.6 shows a microscopic image of a small part of a Holoeye Pluto modulator when displaying the Windows Desktop with the mouse pointer moving. It is clearly visible that

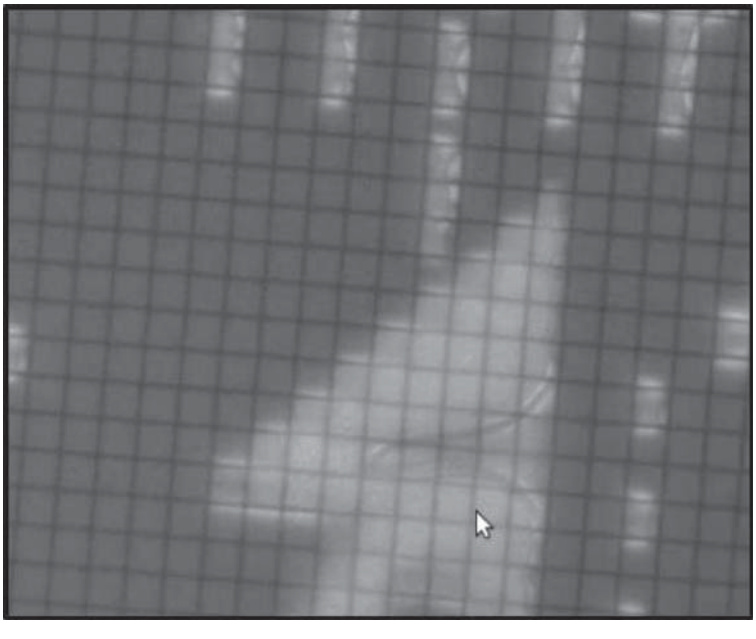

Figure 7.6 Microscopic image of part of a Holoeye Pluto LCoS modulator when displaying the windows desktop with the mouse pointer being moved. Strong fringing field effects as well as effects due to the fuid dynamics of liquid crystal are visible

the individual pixels will not modulate the light in a homogeneous way and that the local behavior of the liquid crystal depends on the local neighborhood as well as on time (see the drag behind the mouse pointer being moved). Especially when used in combination with large carrier frequencies, fringing-field effects become an important source of error. In practically all applications today, such extremely complicated effects are not considered and one lives with the fact that these effects will lead to unwanted diffraction orders and a loss of light in the desired diffraction order (Lingel *et al*. 2013).

7.4 Aberration Correction

Aberration correction is one of the most interesting applications of SLMs in widefield microscopy. The price of the imaging system is strongly correlated with the quality of the employed optics. Furthermore, even if perfect optics are employed, aberrations are often unavoidable in practice due to the specimen itself.

The most important aberration in microscopy (not counting defocus) is spherical aberration (SA) because it is automatically introduced if one focuses into a specimen with the "wrong" refractive index (Booth *et al*. 1998; Booth 2007a; Toeroek *et al*. 1996).

Differernt techniques can be used to reduce or even eliminiate spherical aberration. Most commonly, objectives with correction collars are used. But the adjustment of such collars is a time-consuming manual process (Schwertner *et al*. 2005). Another manual alternative are variable tube-lengths as proposed by Sheppard and Gu (Sheppard and Gu 1991).

But apart from spherical aberration, other aberrations might be present and lead to a deterioration of the image quality. Even small tilts of the cover glass (Arimoto and Murray 2004) have to be considered if the best resolution at high numerical apertures are to be achieved. And, of course, a lot of aberrations are present if one focuses into a thick specimen (Schwertner *et al*. 2004).

7.4.1 Isoplanatic Case

In holographic microscopy (Mico *et al*. 2010; Valencia and Moliner 2010) aberration correction is very simple. Since the complete object wavefront is measured directly (and the image is reconstructed digitally) it is possible to digitally correct the aberrations prior to the reconstruction.

In the following we do not address holographic microscopy any further but concentrate on conventional imaging-based wide-field microscopy. Even there, aberration correction is, in principle, straightforward when using a programmable microscope with the SLM located in a plane conjugate to the pupil. One method for sensing the aberration and one SLM for correcting it is needed. In this case one just writes the conjugate of the aberrated wavefront into the SLM. Therefore, the aberration is canceled and the imaging is improved. Often when implemented with a pixelated light modulator, an additional carrier frequency (phase tilt) as described before, is employed in analogy to conventional off-axis holography. This way the wavefront is coded in the deformation of fringes displayed on the SLM and even binary modulators can be used. In any case, correction is, in principle, very simple and the main challenge is to know the aberration that one has to correct.

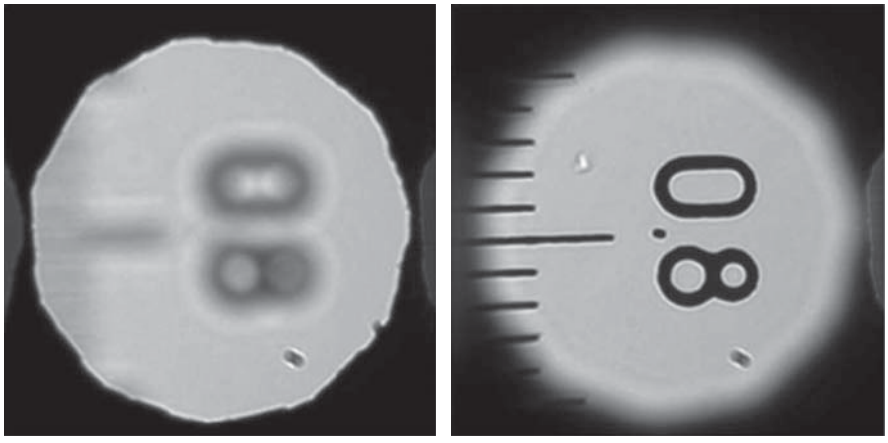

Figure 7.7 Stochastic aberration correction using the method of Warber *et al*. (2010). *Source*: Warber *et al*. 2010. Figure 8. Reproduced with permission from The Optical Society of America (OSA)

Traditionally, standard wavefront sensor concepts are employed but it should be noted that the SLM can also be used to measure aberrations. Different approaches are possible like scene-based Shack–Hartmann sensing (von der Luehe 1988), interference-based methods (Liesener *et al*. 2004c) or direct search-based optimization methods (Liesener *et al*. 2004b). Figure 7.7 shows one example obtained with a system measuring and correcting the aberrations in wide-field microscopy (Warber *et al*. 2010). In combination with microscopic guide stars (Reicherter *et al*. 2004) in principle, a lot of techniques that are also used in astronomic adaptive optics might be employed, for example, Shack–Hartmann sensors, pyramidal sensors (Chamot and Dainty 2006), conoscopic sensors (Buse and Luennemann 2000), curvature sensors (Paterson and Dainty 2000), and phase retrieval methods (Rondeau *et al*. 2007; Teague 1985). Booth *et al*. introduced a modal sensor for microscopy because of the necessity to only correct for lower Zernike orders (Neil *et al*. 2000a,b).

Measurement of the aberrations is quite simple if a single isolated point in the object plane is available. This is the case, for example, in laser scanning microscopy and it becomes possible to completely avoid the wavefront sensor by just optimizing the PSF of the system using an iterative approach. Different algorithms have been proposed to achieve this (Booth 2007b; Liesener *et al*. 2004a; Marsh *et al*. 2003; Sherman *et al*. 2002).

Unfortunately, these methods are not usable for the wide-field microscopic imaging of extended objects because we do not have direct access to the point spread function and only the convolution of the aberrated point spread function with the object to be imaged is detected. The aberration determination is more complicated. Scene-based aberration measurement methods then are to be employed (Bowman *et al*. 2010; Débarre *et al*. 2009; Haist *et al*. 2008; Poyneer 2003; Rimmele *et al*. 2003; von der Luehe 1988; Warber *et al*. 2010).

A simple and straightforward approach is to just correct the aberrations manually (Osten *et al*. 2005; Reicherter *et al*. 2005). For most microscopic applications, which are dominated by only a few low-order terms anyway, this works quite well. Figure 7.8 shows an example of such a correction where diffraction limited imaging could be easily achieved with an SLM microscope, even at high numerical apertures.

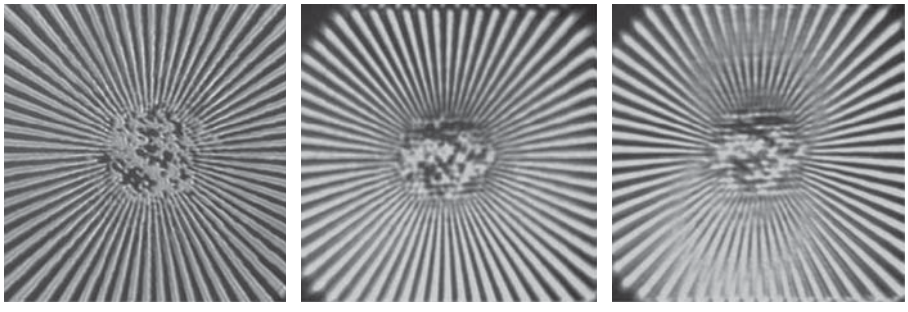

Figure 7.8 Imaging of a Siemens star in transmission with (a) Zeiss Ergoplan (Leitz Wetzlar objective lens, NA = 0.95, l = 540–580 nm) and (b) the SLM microscope (Olympus UmPlanFl objective lens, NA = 0.8, l = 633 nm) with aberration correction, (c) without aberration correction. The half-pitch of the smallest grating structures is 450 nm. *Source*: Hasler *et al.* 2012, Figure 2. Reproduced with permission from The Optical Society of America (OSA)

7.4.2 Field-Dependent Aberrations

A principal problem of aberration correction using the SLM is that the aberration might be field dependent. This is typically the case if the aberration is induced by the specimen itself or by a cheap microscope objective lens. In this case there is not a single wavefront aberration that needs to be corrected so we cannot expect that we will obtain a sharp image over the whole object field.

In a multi-image approach we use different aberration corrections for different field positions, so-called isoplanatic-patches, and the acquired images are then simply combined by digital postprocessing. If the symmetric aberrations are dominating there is no shift in the individual images and therefore no special registration or stitching is necessary to combine the images. One can just copy the corrected areas of different images into one overall image. Figure 7.9 shows an example.

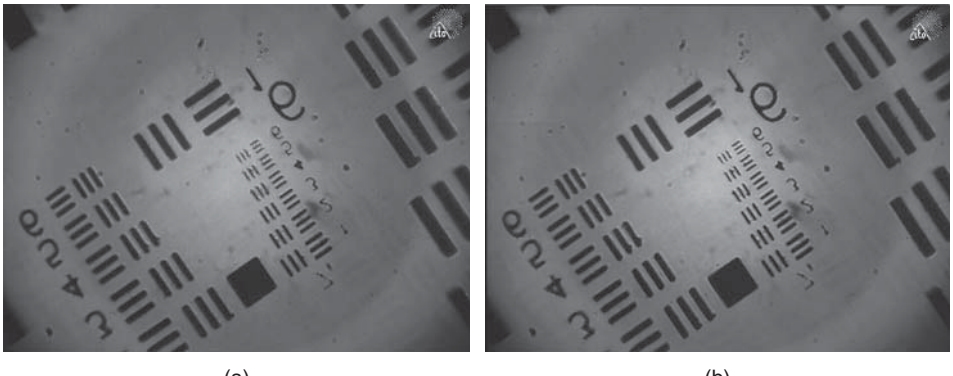

Figure 7.9 Widefield aberration correction using multiple images. (a) single image correction, (b) multi-image correction which leads to multiconjugate adaptive optics

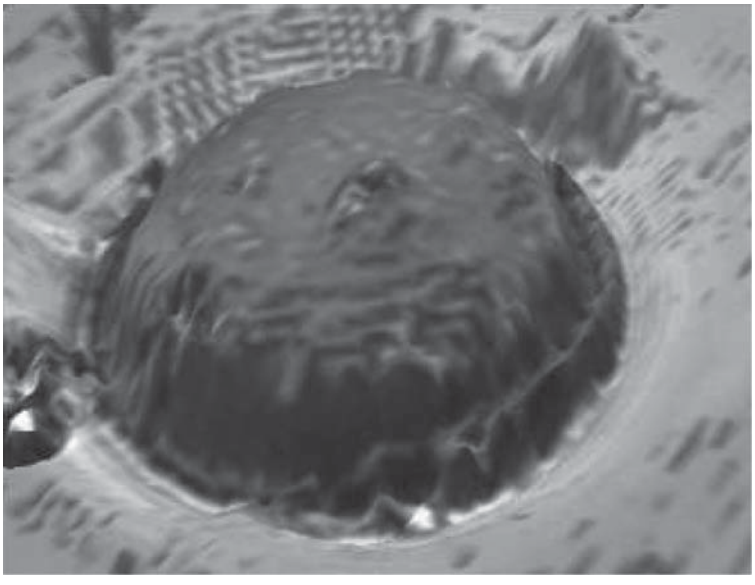

Figure 7.10 Combination of several defocused images allows one to obtain the three-dimensional shape of the specimen

7.4.3 Defocusing

A very special aberration, of course, is defocus. Here, a multi-image approach can be also easily followed using a programmable microscope. We write different zone plates into the SLM and, therefore, different slices of the specimen are sampled. Again, using postprocessing it is possible to combine the images, for example, for obtaining an image with an extended depth of focus, a three-dimensional representation of the object (see e.g., Fig. 7.10), or for visualizing phase objects (Camacho and Zalevsky 2010).

7.5 Phase Contrast Imaging

Most biological (and some important non-biological) specimens are more or less transparent and, therefore, conventional imaging leads to very low contrast. One approach, of course, is to stain the specimen but this might be not convenient and might disturb or even destroy it. Therefore, a lot of different phase contrast techniques have been invented over the years.

In a conventional phase contrast microscope the user has a very limited possibility to change the phase contrast imaging (typically, the phase contrast objective or the bias in differential interference contrast is changed). Programmable microscopy is very much suited to phase contrast imaging, especially in a multi-image context, because one can easily change between different phase contrast methods and their parameters in real time. A good impression of the variance of the images that one obtains by using different phase contrast filters written into the SLM is shown in Fig. 7.11.

Defocusing (compare the previous section), in practice the simplest method of phase contrast filtering, leads to a decrease in lateral resolution. Very small defocusing will not

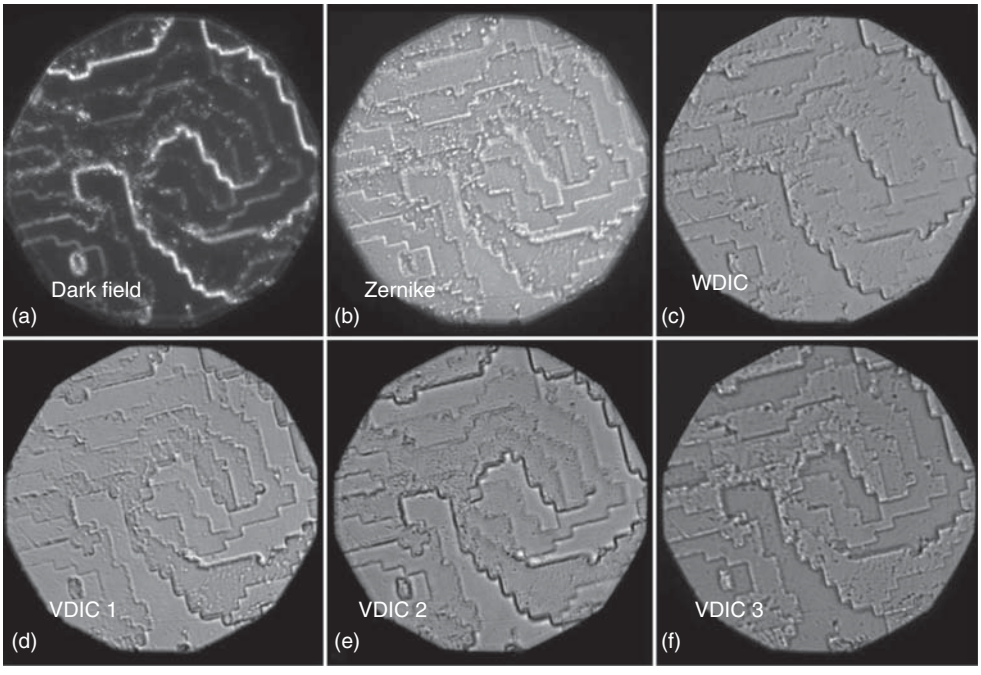

Figure 7.11 Images of a part of a molded computer-generated hologram obtained with different SLM phase contrast settings. *Source*: Warber *et al*. 2011. Figure 6. Reproduced with permission from The Optical Society of America (OSA)

introduce much contrast. But it is an interesting technique when multiple images are used (phase retrieval) and as already described in Section 7.4.3 the defocus can be applied using an SLM (Camacho and Zalevsky 2010).

7.5.1 Dark Field

Conceptually, the most straightforward phase contrast technique is dark field imaging. Despite its simplicity it nevertheless delivers very impressive images for certain applications. The main idea is to block the direct light that will propagate unaffected through the object plane. This means that without a specimen the image on the camera will be dark. To achieve this using a phase modulator, a grating is written into the SLM at all positions that are conjugate to the light source. This way it is possible to direct the unaffected light away from the camera (Fig. 7.12) (Warber *et al*. 2009). Of course, as in conventional microscopy, ring-like or point-like or even more complicated patterns can be employed.

7.5.2 Zernike Phase Contrast

A small variation of the concept leads to Zernike's phase contrast method. In this case the direct light is not blocked but rather shifted in phase. This results in a change of the

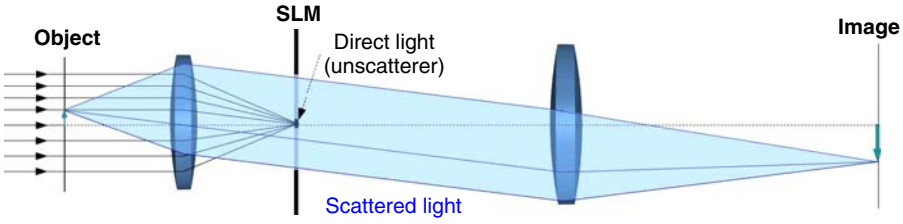

Figure 7.12 Principle of dark field microscopy. Light that is not deflected by structures of the object will be diffracted away from the camera

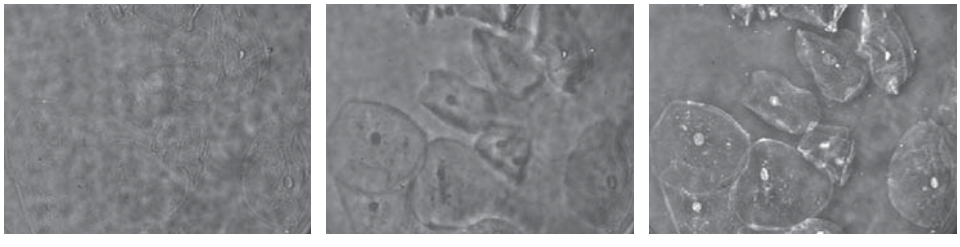

Figure 7.13 Imaging of human mucosa cells using programmable microscopy. (a) bright field image, (b) Zernike setting 1, (c) Zernike setting 2. It is obvious that the character of the image strongly changes if different phase contrast settings are used

interference between the direct light and the light being scattered or diffracted at the object and, therefore, the transparent structures will become visible (Zernike 1955). Compared to conventional Zernike phase contrast the SLM again allows one to change all filter parameters in real time (Glückstad and Mogensen 2001). This allows one to optimize the filter for a given specimen (Fig. 7.13).

As with the dark field technique, one can use more or less arbitrary illumination patterns (Maurer *et al*. 2008). By shifting the phase and recording multiple images it becomes possible to perform even quantitative phase analysis.

7.5.3 Interference Contrast

Apart from the interference between unaffected direct light and scattered light it is also possible to use shearing methods, where the light field coming from the object interferes with a sheared copy of itself. Most common is lateral shearing, which is called *differential interference contrast* (DIC) (Mehta and Sheppard 2008; Pluta 1989). DIC is especially popular in biological research because it can be used even with high numerical aperture (NA) illumination and, therefore, leads to a comparatively good lateral resolution as well as good axial discrimination. Very small features can be imaged with good contrast because the intensity in the image plane is a nonlinear function (approximately a sine squared: Pluta 1989) of the object's phase gradient in the direction of the shear. The shearing in one direction

leads to a pseudo-three-dimensional appearance of phase objects due to a "shadow" in one direction. This can be seen as an advantage or a disadvantage. The effect often is visually very pleasing (and partly responsible for the popularity of DIC) but also leads to loss of information in the direction perpendicular to the shear and the microscope user perceives a three-dimensional topography that might not be real.

Classical DIC is implemented using polarization-based shearing, which unfortunately leads to quite complex and expensive setups. If one only needs quasi-monochromatic imaging, grating-based DIC (David *et al*. 2002; Lohmann and Sinzinger 2006) is an interesting alternative. It can be easily implemented using a programmable microscope, for example, by the complex superposition of two gratings (McIntyre *et al*. 2009b, 2010; Warber *et al*. 2009). Again, all parameters (strength of lateral shear, phase bias between the two copies, shear orientation) can be easily changed in real time.

Sometimes it is also beneficial to replace lateral shear by vertical shearing. To this end the interference between the point image and a defocused point image is used. This leads to the so-called vertical differential interference contrast (Warber *et al*. 2011, 2012).

As with conventional DIC, the results depend strongly on the phase retardation, which in this case is the phase difference between the focused and the slightly defocused part of the point-spread-function. For imaging of neighbouring phase defects the behaviour becomes very complex if spatial coherence in the neighbourhood is given. This is in direct analogy to conventional coherent imaging. Again, the resulting intensity distributions depend strongly on nearly all parameters of the filter and the specimen itself. This is generally the case for interference-based phase contrast imaging of small neighboring structures and makes a good interpretation of such structures sometimes difficult. Therefore, it is a good idea to limit the spatial coherence as much as possible by using a large numerical aperture for illumination.

Figure 7.14 (Plate 12) clearly shows this complexity for the coherent imaging of two neighboring point-like defects using different parameters. By employing the right parameters, the neighbouring defects are clearly separated. It is also obvious that contrast reversal can be achieved using different parameter settings. This can be employed to achieve very strong contrasts by subtracting two recorded images with different parameters (see also Section 7.5.4).

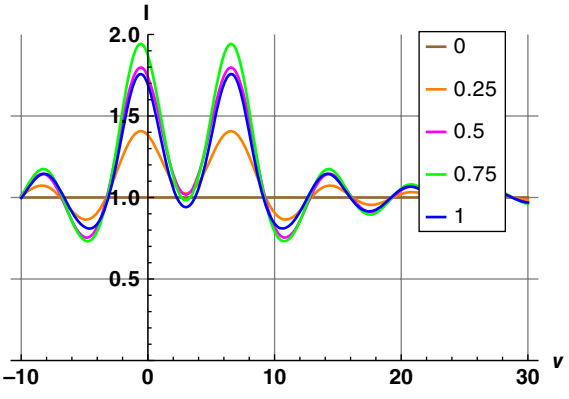

Figure 7.14 (Plate 12) Imaging of two neighboring point-like phase defects using VDIC with different parameters. *See plate section for the color version*

Compared to conventional DIC, the main advantage of VDIC is the isotropy. This eliminates the pseudo-3D like appearance of the images. The images contain more or less the same information but the appearance is different and as such it is also a viable tool to complement other phase contrast methods. Another interesting extension that leads to isotropy, and that can be easily implemented using programmable microscopy, is spiral phase contrast (Bernet *et al*. 2006; Fürhapter *et al*. 2005).

Apart from the mentioned, perhaps most important methods, a lot of other techniques and an endless number of variations are possible.

7.5.4 Combining Different Phase Contrast Images

We have already seen that the phase contrast images strongly depend on the method, the parameters of the method, and the specimen itself. It is clear that by combining images, which have been obtained using different parameter sets or different methods, this might improve the visibility of structures or make the enclosed information more visible. This approach is technically very attractive because it is so easy to combine the images. The images have been obtained with the same static optical setup and on the same CCD. Therefore, no registration or stitching is necessary. Every object detail stays at exactly the same pixel (at least while the object itself is not moving).

One example is shown in Fig. 7.15 (Plate 13). Here, two images obtained using Zernike's phase contrast and DIC are combined by postprocessing. Zernike's method is sensitive to the

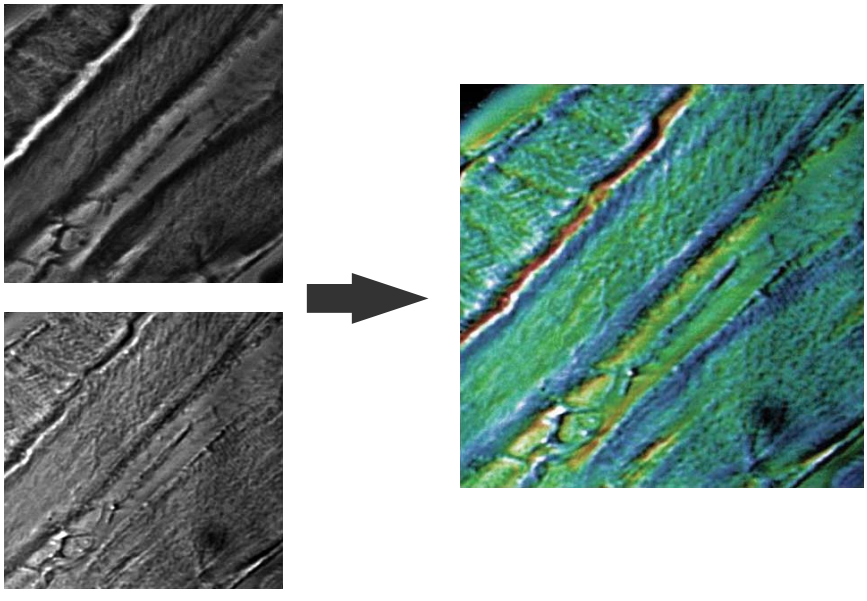

Figure 7.15 (Plate 13) Combination of an image obtained using Zernike phase contrast (hue) and one obtained using DIC (intensity) in order to visualize a phase structure. *See plate section for the color version*

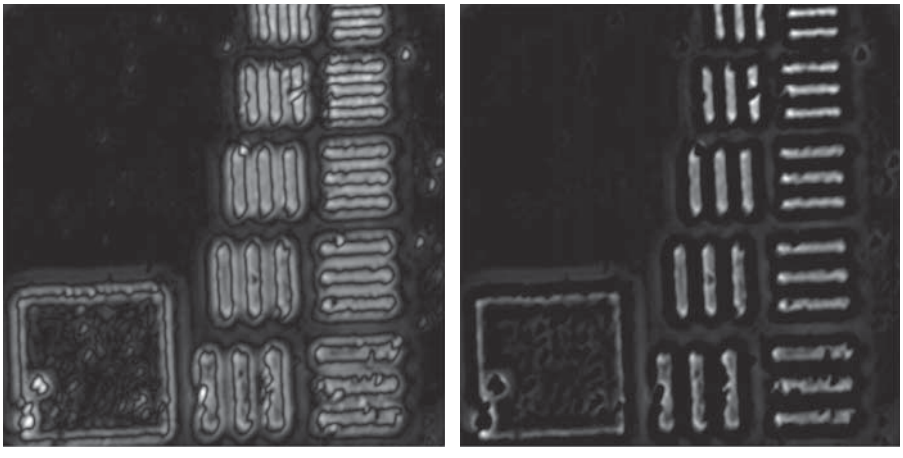

(a) (b)

Figure 7.16 Combination of two VDIC images when imaging part of a three-bar binary phase target. (a) The dark contours surounding the bars are precise indicators for the lateral extension of the structures. (b) Strong contrast improvement for the structure. *Source*: Warber *et al*. 2011. Figure 7. Reproduced with permission from The Optical Society

phase of the object. For an object consisting of more or less homogeneous material the phase is proportional to the local thickness. DIC, on the other hand, is sensitive to the gradient of the phase and is therefore very well suited to enhance small structures. In Fig. 7.15 we therefore used the Zernike image for the hue and the DIC image for the intensity of a color image. This way color is related to the local height.

Another example is shown in Fig. 7.16 where an USAF phase target has been imaged using two different sets of parameters of VDIC. The subtraction of the two images leads to a strongly increased contrast.

7.6 Stereo Microscopy

In stereo microscopy the specimen is imaged from two different directions. The angle between the two directions is the so-called triangulation angle. Practically, this can be achieved in programmable microscopy by using two (or even more) different zones of the pupil of the system. Figure 7.17 depicts the basic idea (Hasler *et al*. 2012).

On the left part of the pupil we use a grating displayed on the left part of the SLM. Therefore, the light which falls onto that side of the pupil will form an image that is shifted with respect to the image due to the right part of the image. On the camera, we therefore will have two separated copies of the object. We can use these two images for visualization (e.g., sending them to a 3D display) or for computing the topography of the object using stereo-vision algorithms.

For transparent objects, unfortunately, we might obtain local contrast reversals. Therefore, for phase contrast imaging, stereo-based microscopy techniques at the moment do not lead to satisfactory results.

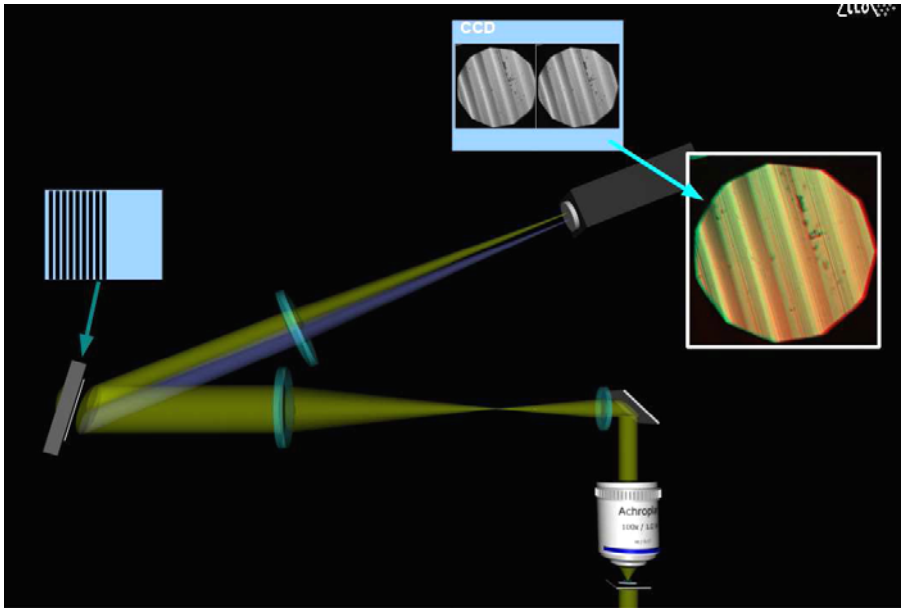

Figure 7.17 Principle of SLM-based stereo microscopy

7.7 Conclusion

We have reviewed different multidimensional imaging methods implemented using SLM-based programmable microscopy. By incorporating a spatial light modulator into the imaging path of a microscope it becomes possible to realize a lot of different imaging methods by software. Due to the possibility of addressing the SLM in video real time one can obtain images obtained with different microscopy methods and different parameters very fast and it is possible to combine these images by postprocessing.

Apart from the optimization of parameters and imaging methods, we have shown multi-image advantages for the optimization of the imaging quality (field-dependent aberrations, multiconjugate adaptive optics), contrast enhancement of phase contrast images, improved visualization of phase specimen, and three-dimensional registration of objects.

At the moment we only scratched at the surface of the possibilities. A wealth of new imaging capabilities will arise if one really exploits the power of postprocessing in a more thorough way. We also only used the spatial light modulator in the imaging path of the microscope. As we have shown in Section 7.2 it is also possible to use spatial light modulation in the illumination path of the microscope. This way, even more imaging methods can be achieved in a flexible way by programming the SLM. Important methods are confocal-like, structured-illumination techniques, and special illumination methods, for example, for Raman- or fluorescence-based imaging.

The disadvantages of SLM-based microscopy are the reduced light efficiency of the microscope and – for most methods – the limitation to quasi-monochromatic light. Still, we think that part of the future of microscopy lies in this sort of multi-image generation and combination by postprocessing, which is enabled by the enormous flexibility of programmable microscopy.

References

Arimoto R and Murray JM 2004 A common aberration with water-immersion objective lenses. *Journal of Microscopy* **216**(1), 49–51.

Bernet S, Jesacher A, Maurer C and Ritsch-Marte M 2006 Quantitative imaging of complex samples by spiral phase contrast microscopy. *Optics Express* **14**(9), 2766–2773.

Booth M, Neil M and Wilson T 1998 Aberration correction for confocal imaging in refractive-index-mismatched media. *Journal of Microscopy* **192**, 90–98.

Booth MJ 2007a Adaptive optics in microscopy. *Philosophical Transactions. Series A, Mathematical, Physical, and Engineering Sciences* **365**(1861), 2829–2843.

Booth MJ 2007b Wavefront sensorless adaptive optics for large aberrations. *Optics lett*, **32**(1), 5–7.

Bowman RW, Wright AJ and Padgett MJ 2010 An SLM-based shack-hartmann wavefront sensor for aberration correction in optical tweezers. *Journal of Optics* **12**(12), 124004.

Buse K and Luennemann M 2000 3D imaging: Wave front sensing utilizing a birefrigent crystal. *Phyical Review Letters* **85**, 3385–3387.

Camacho L and Zalevsky Z 2010 Quantitative phase microscopy using defocusing by means of a spatial light modulator. *Optics Express* **18**(7), 6755–6766.

Chamot S and Dainty C 2006 Adaptive optics for ophtalmic applications using a pyramid wavefront sensor. *Optics Express* **14**, 518–526.

Chang B, Chou L, Chang Y and Chiang S 2009 Isotropic image in structured illumination microscopy patterned with a spatial light modulator. *Optics Express* **17**(17), 8206–8210.

Choi Jr and Kim D 2012 Enhanced image reconstruction of three-dimensional fluorescent assays by subtractive structured-light illumination microscopy. *J Opt Soc Am A Opt Image Sci Vis.* **29**(10), 2165–2173.

David C, Nohammer B, Solak HH and Ziegler E 2002 Differential x-ray phase contrast imaging using a shearing interferometer. *Applied Physics Letters* **81**(17), 3287.

Débarre D, Botcherby EJ, Watanabe T, Srinivas S, Booth MJ and Wilson T 2009 Image-based adaptive optics for two-photon microscopy. *Optics Lett.* **34**(16), 2495–2497.

Eriksen RL, Mogensen PC and Glückstad J 2002 Multiple-beam optical tweezers generated by the generalized phase-contrast method. *Opt. Letters* **27**(4), 267–269.

Fürhapter S, Jesacher A, Bernet S and Ritsch-Marte M 2005 Spiral phase contrast imaging in microscopy. *Optics Express* **13**(3), 689–694.

Gittard SD, Nguyen A, Obata K, Koroleva A, Narayan RJ and Chichkov BN 2011 Fabrication of microscale medical devices by two-photon polymerization with multiple foci via a spatial light modulator. *Optics Express* **2**(11), 267–275.

Glückstad J and Mogensen PC 2001 Optimal phase contrast in common-path interferometry. *Applied Optics* **40**(2), 268–282.

Grier D 2003 A revolution in optical manipulation. *Nature* **424**, 810–816.

Haist T, Hafner J, Warber M and Osten W 2008 Scene-based wavefront correction with spatial light modulators *Proceedings of SPIE*, vol. **7064**, pp. 70640M–70640M–11. SPIE.

Haist T, Wagemann EU and Tiziani HJ 1999 Pulsed-laser ablation using dynamic computer-generated holograms written into a liquid crystal display. *Journal of Optics A: Pure and Applied Optics* **1**(3), 428–430.

Hasler M, Haist T and Osten W 2012 Stereo vision in spatial-light-modulator–based microscopy. *Opt. Lett.* **37**(12), 2238–2240.

Hayasaki Y, Itoh M, Yatagai T and Nishida N 1999 Nonmechanical optical manipulation of microparticle using spatial light modulator. *Optical Review* **6**(1), 24–27.

Heintzmann R, Hanley QS, Arndt-Jovin D and Jovin TM 2001 A dual path programmable array microscope (PAM): simultaneous acquisition of conjugate and non-conjugate images. *Journal of Microscopy* **204**(Pt 2), 119–35.

Hussain A and Campos J 2013 Holographic superresolution using spatial light modulator. *Journal of the European Optical Society - Rapid Publications* 8, DOI: 10.2971/jeos.2013.13007.

Jesacher A and Booth MJ 2010 Parallel direct laser writing in three dimensions with spatially dependent aberration correction. *Optics Express* **18**(20), 132–134.

Jesacher A, Roider C, Khan S, Thalhammer G, Bernet S and Ritsch-Marte M 2011 Contrast enhancement in widefield CARS microscopy by tailored phase matching using a spatial light modulator. *Optics Lett.* **36**(12), 2245–2247.

Kenny F, Lara D and Dainty C 2012 Complete polarization and phase control for focus-shaping in high-NA microscopy. *Optics Express* **20**(13), 2234–2239.

Khan S, Jesacher A, Nussbaumer W, Bernet S and Ritsch-Marte M 2011 Quantitative analysis of shape and volume changes in activated thrombocytes in real time by single-shot spatial light modulator-based differential interference contrast imaging. *Journal of Biophotonics* **4**(9), 600–609.

Kim T and Popescu G 2011 Laplace field microscopy for label-free imaging of dynamic biological structures. *Optics Letters* **36**(23), 4704–4706.

Lazarev G, Hermerschmidt A, Krüger S and Osten S 2012 LCOS Spatial light modulators: trends and applications. *in Optical Imaging and Metrology*, W. Osten, N. Reingang (eds), Springer. pp. 1–23.

Lee MP, Gibson GM, Bowman R, Bernet S, Ritsch-Marte M, Phillips DB and Padgett MJ 2013 A multi-modal stereo microscope based on a spatial light modulator. *Opt. Express* **21**(14), 16541–16551.

Liang J, Wu SY, Fatemi FK and Becker MF 2012 Suppression of the zero-order diffracted beam from a pixelated spatial light modulator by phase compression. *Appl. Opt.* **51**(16), 3294–3304.

Liesener J, Hupfer W, Gehner A and Wallace K 2004a Tests on micromirror arrays for adaptive optics. *Proc. SPIE*.

Liesener J, Reicherter M and Tiziani H 2004b Determination and compensation of aberrations using SLMs. *Optics Communications* **233**, 161–166.

Liesener J, Seifert L, Tiziani H and Osten W 2004c Active wavefront sensing and wavefront control with SLMs. *Proc. SPIE* **5532**(1), 147–158.

Lingel C, Haist T and Osten W 2013 Optimizing the diffraction efficiency of SLM-based holography with respect to the fringing field effect. *Appl. Opt.* **52**(28), 6877–6883.

Lohmann A and Sinzinger S 2006 *Optical Information Processing*. TU Illmenau Universitätsbibliothek.

Marsh P, Burns D and Girkin J 2003 Practical implementation of adaptive optics in multiphoton microscopy. *Opt. Express* **11**, 1123–1130.

Maurer C, Jesacher A, Bernet S and Ritsch-Marte M 2008 Phase contrast microscopy with full numerical aperture illumination. *Optics Express* **16**(24), 19821–19829.

Maurer C, Jesacher A, Bernet S and Ritsch-Marte M 2011 What spatial light modulators can do for optical microscopy. *Laser & Photonics Reviews* **5**(1), 81–101.

McIntyre TJ, Maurer C, Bernet S and Ritsch-Marte M 2009a Differential interference contrast imaging using a spatial light modulator. *Optics Lett.* **34**(19), 2988–2990.

McIntyre TJ, Maurer C, Bernet S and Ritsch-Marte M 2009b Differential interference contrast imaging using a spatial light modulator. *Opt. Lett.* **34**(19), 2988–2990.

McIntyre TJ, Maurer C, Fassl S, Khan S, Bernet S and Ritsch-Marte M 2010 Quantitative SLM-based differential interference contrast imaging. *Optics Express* **18**(13), 14063–14078.

Mehta SB and Sheppard CJR 2008 Partially coherent image formation in differential interference contrast (DIC) microscope. *Optics Express* **16**(24), 19462–19479.

Mico V, Garcia J, Zalevsky Z and Javidi B 2010 Phase-shifting Gabor holographic microscopy. *Journal of Display Technology* **6**(10), 484–489.

Neil Ma, Booth MJ and Wilson T 2000a Closed-loop aberration correction by use of a modal Zernike wave-front sensor. *Optics lett*, **25**(15), 1083–1085.

Neil Ma, Juskaitis R, Booth MJ, Wilson T, Tanaka T and Kawata S 2000b Adaptive aberration correction in a two-photon microscope. *Journal of Microscopy* **200** (Pt 2)(July), 105–108.

Nikolenko V, Peterka DS and Yuste R 2010 A portable laser photostimulation and imaging microscope. *Journal of Neural Engineering* **7**(4), 045001.

Nikolenko V, Watson BO, Araya R, Woodruff A, Peterka DS and Yuste R 2008 SLM microscopy: Scanless two-photon imaging and photostimulation with spatial light modulators. *Front Neural Circuits* **2**, 5.

Olivier S 2007 Adaptive optics. *in "Micro-Opto-Electro-Mechanical Systems",* ME Motamedi (ed.) SPIE Press Book. pp. 453–475.

Osten W, Kohler C and Liesener J 2005 Evaluation and application of spatial light modulators for optical metrology *a Reunion Espanola de Optoelectronica OPTOEL '05, Elche, Spain*.

Paterson C and Dainty JC 2000 Hybrid curvature and gradient wave-front sensor. *Opt. Lett.* **25**(23), 1687–1689.

Paterson C, Munro I and Dainty J 2000 A low cost adaptive optics system using a membrane mirror. *Optics Express* **6**, 175–185.

Peterka DS, Nikolenko V, Fino E, Araya R, Etchenique R, Yuste R, *et al*. 2010 Fast two-photon neuronal imaging and control using a spatial light modulator and ruthenium compounds. *Library* **7548**, 1–9.

Pham H, Bhaduri B, Ding H and Popescu G 2012 Spectroscopic diffraction phase microscopy. *Optics Lett.* **37**(16), 3438–3440.

Pluta M 1989 *Advanced Light Microscopy Vol. 2*. Elsevier.

Poyneer La 2003 Scene-based Shack–Hartmann wave-front sensing: analysis and simulation. *Applied Optics* **42**(29), 5807–5815.

Qin W, Shao Y, Liu H, Peng X, Niu H and Gao B 2012 Addressable discrete-line-scanning multiphoton microscopy based on a spatial light modulator. *Optics Lett.* **37**(5), 827–829.

Reicherter M, Gorski W, Haist T and Osten W 2004 Dynamic correction of aberrations in microscopic imaging systems using an artificial point source. *SPIE-Int. Soc. Opt. Eng. Proceedings of Spie–the International Society for Optical Engineering* **5462**(1), 68–78.

Reicherter M, Haist T, Wagemann EU and Tiziani HJ 1999 Optical particle trapping with computer-generated holograms written on a liquid-crystal display. *Optics Lett.* **24**(9), 608.

Reicherter M, Haist T, Zwick S, Burla A, Seifert L and Osten W 2005 Fast hologram computation and aberration control for holographic tweezers. *Proceedings of SPIE* **5930**, Optical Trapping and Optical Micromanipulation II, 59301Y.

Rimmele T, Richards K, Hegwer S, Ren D, Fletcher S, Gregory S, *et al*. 2003 Solar adaptive optics: A progress report. *Proc. SPIE.* **4839**, Adaptive Optical System Technologies II, 635

Rondeau X, Thiebaut E, Tallon M and Foy R 2007 Phase retrieval from speckle images. *J. Opt. Soc. Am. A* **24**, 3354–3364.

Schausberger SE, Heise B, Maurer C, Bernet S, Ritsch-Marte M and Stifter D 2010 Flexible contrast for low-coherence interference microscopy by Fourier-plane filtering with a spatial light modulator. *Optics Letters* **35**(24), 4154–4156.

Schwertner M, Booth M and Wilson T 2005 Simple optimization procedure for objective lens correction collar setting. *Journal of Microscopy* **217**, 184–1887.

Schwertner M, Booth MJ and Wilson T 2004 Simulation of specimen-induced aberrations for objects with spherical and cylindrical symmetry. *Journal of Microscopy* **215**(Pt 3), 271–280.

Scrimgeour J and Curtis JE 2012 Aberration correction in wide-field fluorescence microscopy by segmented-pupil image interferometry. *Optics Express* **20**(13), 388–394.

Shao Y, Qin W, Liu H, Qu J, Peng X, Niu H and Gao BZ 2012 Ultrafast, large-field multiphoton microscopy based on an acousto-optic deflector and a spatial light modulator. *Optics Lett.* **37**(13), 2532–2534.

Sheppard CRJ and Gu M 1991 Aberration compensation in confocal microscopy. *Applied Optics* **30**, 3563–3568.

Sherman L, J.Y. Y, Norris A and T.B. N 2002 Adaptive correction of depth-induced aberrations in multiphoton scanning microscopy using a deformable mirror. *Journal of Microscopy* **206**, 65–71.

Steiger R, Bernet S and Ritsch-Marte M 2012 SLM-based off-axis Fourier filtering in microscopy with white light illumination. *Optics Express* **20**(14), 15377–15384.

Teague MR 1985 Image formation in terms of the transport equation. *J. Opt. Soc. Am. A* **2**(11), 1434.

Toeroek P, Sheppard C and Laczik Z 1996 Dark-field and differential phase contrast imaging modes in confocal microscopy using a half-aperture stop. *Optik* **103**(3), 101–106.

Tyson R 1998 *Principles of Adaptive Optics,* Academic Press.

Valencia UD and Moliner D 2010 Common-path phase-shifting lensless holographic microscopy. *Optics Lett.* **35**(23), 3919–3921.

von der Luehe O 1988 Wavefront error measurement technique using extended, incoherent light sources. *Optical Engineering* **27**(12), 1078–1087.

Wang Cc, Lee Kl and Lee Ch 2009 Wide-field optical nanoprofilometry using structured illumination. *Optics Lett.* **34**(22), 3538–3540.

Warber M, Haist T, Hasler M and Osten W 2012 Vertical differential interference contrast. *Optical Engineering* **51**(1), 013204–1–013204–7.

Warber M, Hasler M, Haist T and Osten W 2011 Vertical differential interference contrast using SLMs. *Proc. SPIE* **8086**, 80861E–80861E–10.

Warber M, Maier S, Haist T and Osten W 2010 Combination of scene-based and stochastic measurement for wide-field aberration correction in microscopic imaging. *Applied Optics* **49**(28), 5474–5479.

Warber M, Zwick S, Hasler M, Haist T and Osten W 2009 SLM-based phase-contrast filtering for single and multiple image acquisition. *Proc SPIE* **7442**, Optics and Photonics for Information Processing III, 74420E.

Zernike F 1955 How I discovered phase contrast. *Science* **121**(3141), 345–349.

Zhou Q, Yang W, He F, Stoian R, Hui R and Cheng G 2013 Femtosecond multi-beam interference lithography based on dynamic wavefront engineering. *Optics Express* **21**(8), 53–56.

Zwick S, Haist T, Warber M and Osten W 2010 Dynamic holography using pixelated light modulators. 7.1 *Applied Optics* **49**(25), F47–58.